

Review

# Molecularly Imprinted Polymers for Chemical Sensing: A Tutorial Review

Nadja Leibl<sup>1,2</sup>, Karsten Haupt<sup>1</sup>, Carlo Gonzato<sup>1,\*</sup> and Luminita Duma<sup>1,\*</sup> 

<sup>1</sup> CNRS Enzyme and Cell Engineering Laboratory, Université de Technologie de Compiègne, Sorbonne Universités, Rue du Docteur Schweitzer, CS 60319, CEDEX, 60203 Compiègne, France; nadja.leibl@airbus.com (N.L.); karsten.haupt@utc.fr (K.H.)

<sup>2</sup> APSYS—An Airbus Company, ZI de Couperigne CTMA Bat B, 13127 Vitrolles, France

\* Correspondence: carlo.gonzato@utc.fr (C.G.); luminita.duma@utc.fr (L.D.)

**Abstract:** The field of molecularly imprinted polymer (MIP)-based chemosensors has been experiencing constant growth for several decades. Since the beginning, their continuous development has been driven by the need for simple devices with optimum selectivity for the detection of various compounds in fields such as medical diagnosis, environmental and industrial monitoring, food and toxicological analysis, and, more recently, the detection of traces of explosives or their precursors. This review presents an overview of the main research efforts made so far for the development of MIP-based chemosensors, critically discusses the pros and cons, and gives perspectives for further developments in this field.

**Keywords:** molecularly imprinted polymers; chemosensors; sensors



**Citation:** Leibl, N.; Haupt, K.; Gonzato, C.; Duma, L. Molecularly Imprinted Polymers for Chemical Sensing: A Tutorial Review. *Chemosensors* **2021**, *9*, 123. <https://doi.org/10.3390/chemosensors9060123>

Academic Editor: Chung-Wei Kung

Received: 14 April 2021

Accepted: 20 May 2021

Published: 26 May 2021

**Publisher's Note:** MDPI stays neutral with regard to jurisdictional claims in published maps and institutional affiliations.



**Copyright:** © 2021 by the authors. Licensee MDPI, Basel, Switzerland. This article is an open access article distributed under the terms and conditions of the Creative Commons Attribution (CC BY) license (<https://creativecommons.org/licenses/by/4.0/>).

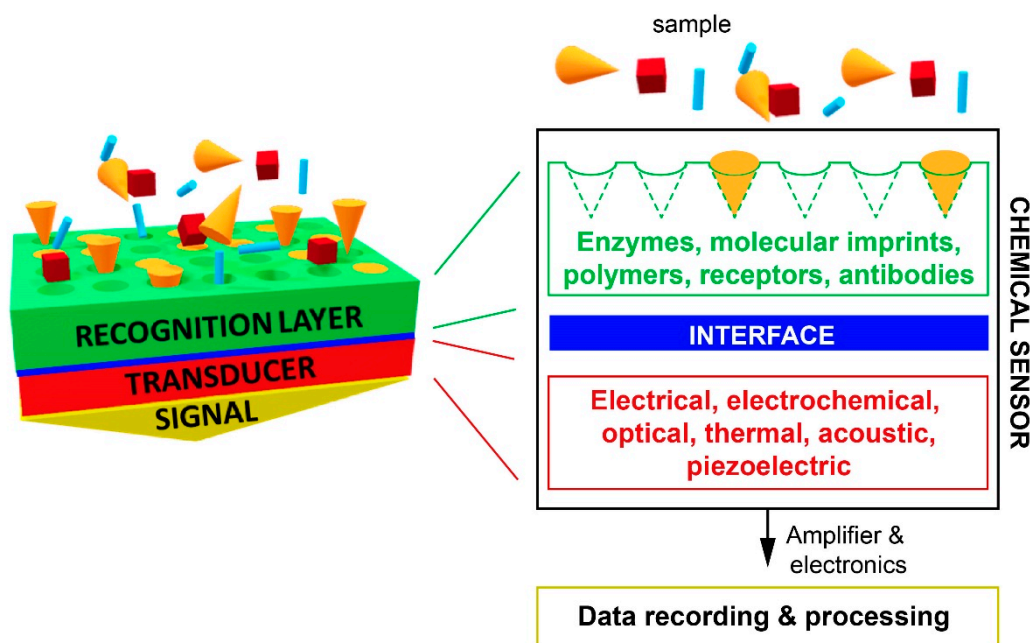
## 1. Introduction

Molecularly imprinted polymers (MIPs) have seen a continuous development as sensing elements in bio-/chemo-sensors since the late 1990s [1–6]. MIPs are attractive not only for their recognition properties that are close to those of natural receptors and their availability for a wide range of targets but also for their superior chemical and physical stability compared to biological receptors. These advantages have led to the application of MIPs in fields as various as immunoassays, separation, depollution, sensing, cell imaging, and therapy [7–9]. The imprinting process consists of polymerizing functional and cross-linking monomers in the presence of a template. The removal of the later leaves cavities complementary in shape, size, and chemical functionality, therefore allowing for the template to rebind specifically.

According to the International Union of Pure and Applied Chemistry (IUPAC), a chemical sensor is “a device that transforms chemical information, ranging from the concentration of a specific sample component to total composition analysis, into an analytically useful signal. The chemical information, mentioned above, may originate from a chemical reaction of the analyte or from a physical property of the system investigated” [10]. Therefore, a suitable sensor has to fulfil specific criteria such as high sensitivity and selectivity, stability, low sample consumption, reliability, and reproducibility. Overall, an ideal sensor should also be inexpensive, portable, foolproof, able to instantaneously respond to the analyte of interest in any desired medium, and capable of generating a measurable signal in the required concentration range. Unfortunately, current sensors are far from being “ideal”, and chemical sensors in particular are generally narrowly optimized for a given application [11,12].

As mentioned above, a chemical sensor consists of two main elements (see Scheme 1): the chemical recognition element, called the receptor, and a physico-chemical transducer. The receptor transforms the binding event of the target into a form of energy that can be measured by the transducer. For chemical sensors, this binding event involves chemical

species and the generation of a signal upon the change of a physico-chemical parameter (e.g., the formation/breaking of a bond, exchange of electrons, and mass change or refractive index modification). Subsequently, the transducer transforms the chemical information received from the receptor into a useful analytical signal. The transduction process can be based on several physical phenomena, such as optical or thermal changes, electrochemical reactions, and mass variations.



**Scheme 1.** Scheme of a chemical sensor consisting of a recognition layer, an interface, a transducer, and a signal detection element.

As a recent trend, the miniaturization of sensors and their readout deserves a special attention due to the increasing number of applications available for smartphones [13–17]. From a general point of view, receptor design is perhaps the crucial step in the process of sensor development because it has to match the requirements of high selectivity and sensitivity for a target with the particular characteristics of a given readout. Thus, the straightforward engineering, fine-tuning, and easiness of integration into the standard industrial process of MIPs makes them ideal candidates for recognition elements.

In this review, we describe the current state of the research field on MIP-based electrochemical, mass-sensitive, and optical sensors, and we highlight their advantages and shortcomings. The last section discusses aspects related to chemical interfacing in the design of MIP-based chemosensors. Reviews from 2020 and 2021 already described various characteristics related to MIP synthesis and the readout mode of MIP-based potentiometric sensors for the detection of organic and biological species [18], the advantages of nanomaterial-based MIPs for pesticides sensing [19], and the strength/weakness ratio for potentiometric sensors in general [20], which are not tackled in this work.

## 2. Electrochemical MIP Sensors

Electrochemical sensors represent one of the most successfully applied MIP-based sensors [21–25]. Electrochemical sensors are defined as devices wherein a sensing layer is coupled to an electrochemical transducer [26]. Depending on the electrical phenomenon used for transducing the binding event, different families of electrochemical sensors can be distinguished: potentiometric (sensing a change in the membrane potential), conductometric (conductance variation), impedimetric (impedance fluctuation), and voltammetric or amperometric (overall current variation induced either by an electrochemical reaction upon a voltage switch or a time-dependent evolution over a constant potential, respectively) [27].

In the early 1990s, Mosbach and coworkers reported the first use of MIPs for the capacitive [28] or amperometric [21] detection of L-phenylalanine and morphine. Already in these early works, it became clear that the different transduction methods dictated the requirements for the suitable interfacing of the MIP. A major drawback of the most commonly used (meth)acrylate-based MIPs was their nonconductive nature; therefore, they were combined with electrically conductive polymers that remarkably improved the transduction [22]. Many valuable reviews have covered the wide range of applications of electrochemical MIP sensors [27,29–31], and they are therefore not discussed in detail here.

Electrochemical devices are classified depending on the reaction under study (amperometric, potentiometric and conductometric sensors) or depending on the detection technique (impedimetric or field-effect sensors) [32]. As a result, the reaction generates different types of signals: (i) a measurable current for amperometric sensors, (ii) a measurable potential or charge accumulation for potentiometric sensors, and (iii) a measurable alteration of the conductive properties for conductometric sensors. Impedimetric sensors measure the impedance based on both resistance and reactance effects [33], whereas field-effect devices quantify the current induced by a potentiometric effect at a gate electrode in a transistor [26].

### 2.1. Potentiometric Sensors

Among the different chemical sensors, potentiometric sensors are the most popular due to their low cost and easy handling. This type of sensor works in the near-zero current flow, measuring the difference in potential between a working electrode (WE) and a reference electrode (RE), which generates an analytical signal. Ion selective electrodes (ISEs), which use a permselective membrane able to produce a potential in contact with solutions of a given analyte, are a prominent example of this class of transducers. The most known examples are glass electrodes for pH measurements. The membrane, which consists of a lipophilic-complexing agent that selectively binds the analyte of interest, is the key component.

When moving to MIP-based systems, potentiometric sensors represent a well-established class. For these sensors, low conductivity, hydrophobicity, and high selectivity are all requirements that (meth)acrylate-MIPs fit perfectly. Two different kinds of potentiometric sensors can be distinguished. The first comprises faradaic coupled devices (with a conventional inner-reference ISE; see Figure 1a) and capacitive coupled devices (with solid inner contacts, coated wire ISE; see Figure 1b), and the second comprises an ion-sensitive field-effect transistors (ISFETs).

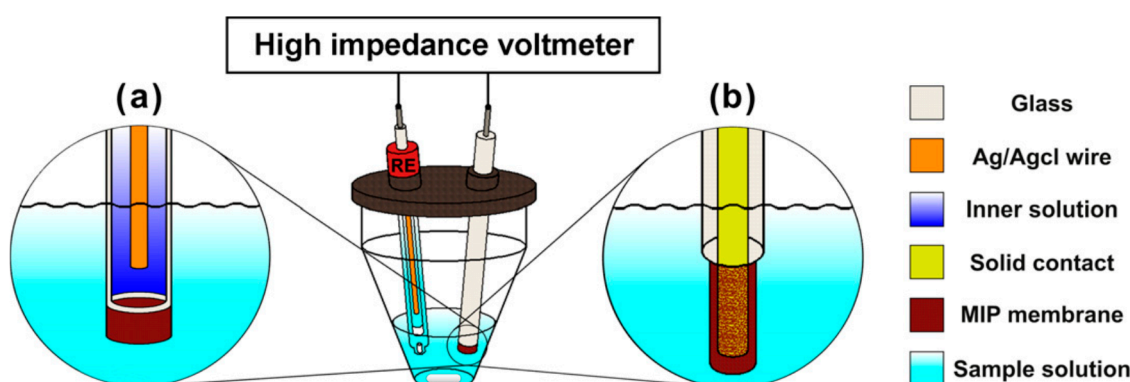


**Figure 1.** Typical setup for potentiometric measurements: with either an inner-reference ion-selective electrode (ISE) (a) or coated wire ISE (b) and a reference electrode (RE). Reprinted with permission from [27].

The classical setup is a faradaic coupled device in which the permselective membrane separates two compartments with solutions of different activity for a given ion (the sample and the internal electrolyte solution). Approaches similar to those of conventional ISEs are used to incorporate MIPs into the membranes as selective ionophores by embedding

imprinted particles into a polymer matrix, typically polyvinylchloride (PVC). These have been referred to as “imprinted polymer inclusion membranes” [34]. Such membranes have been reported for the detection of dysprosium (III) and other lanthanides [35], as well as for the pesticide atrazine [36] and melamine in milk [22]. Their response greatly depends on how the membrane is tailored, e.g., the presence of ionic additives and the type and amount of the added plasticizer and MIP.

In addition to faradaic potentiometric sensors, capacitive sensors are also well-established. In contrast to the former, capacitive sensors do not use an inner solution, as the ion-selective membrane is directly in contact with a solid phase and the sample. The solid contact consists of conductors, semi-conductors, or insulators. This type of sensor can be further split into two subgroups, with either the membrane parallel to the coated wire electrodes or with a field-effect transistor device. For the development of solid-contact potentiometric sensors, conductive polymers are a clear advantage. A polymer coating is usually achieved by either the electropolymerization of MIPs (e.g., polypyrrole) or by the drop-casting of pre-synthesized acrylic MIPs embedded in plasticized PVC matrixes (as described before) on noble metals (such as Pt and Au) or carbon material (such as glassy carbon and graphite) for coated wire electrodes. The capacitive readout is based on the ionic charge-transfer occurring on the membrane in the presence of an analyte. Such coated electrodes have been used for sensing various compounds: nitrates [37], pesticides [38], antibiotics [39], and  $\beta$ -blockers [40]. Table 1 summarizes the type of MIP, the analyte, the limit of detection (LOD), and, when available, the response time and stability of the sensors for the detection of these analytes. Another important way to obtain a selective electrode is by mixing a MIP-based membrane with carbon paste (e.g., graphite powder) [41] or relying on self-assembled monolayers (SAMs) [42]. For the second subgroup, ion-sensitive field-effect transistors are the most common examples. In this case, the ion-selective membrane is deposited onto the input dielectric of the field-effect transistor. Examples of target analytes for these are chloroaromatic acids [43], nucleotides and various acids [44,45], thiophenols [45], and NAD(P)<sup>+</sup>/NAD(P)H cofactors [46] (see Table 1). The development of such potentiometric sensors led to the fabrication of a platform consisting of the sensor and the readout circuit in one device called a microelectromechanical system (MEMS) [47], which is particularly interesting for the miniaturization and, thus, for mass-production of commercial sensing devices. An emerging field in the development of MIP-based potentiometric sensors is the replacement of expensive gold or glassy carbon electrode substrates by commercially-available, low-cost chromatography paper [48]. The paper sensor selective for bisphenol A showed a comparable analytical performance to a classical glassy carbon-based sensor. The detection limit was 0.15  $\mu$ M (see Table 1), with good selectivity over other phenols.

**Table 1.** MIP-based electrochemical sensors.

| Transducer     | Receptor                        | Analyte                      | LOD (mol/L)          | Response Time (s) | Stability (Weeks) | Ref  |
|----------------|---------------------------------|------------------------------|----------------------|-------------------|-------------------|------|
| Potentiometric | MIPs                            | Nitrates                     | $0.2 \times 10^{-6}$ | 24                | -                 | [37] |
|                | MIPs into membranes             | Dy(III)                      | $2 \times 10^{-6}$   | 10                | -                 | [35] |
|                |                                 | Atrazine                     | $0.5 \times 10^{-6}$ | 120               | -                 | [36] |
|                |                                 | Melamine                     | $5 \times 10^{-6}$   | 16                | -                 | [22] |
|                |                                 | NAD(P) <sup>+</sup> /NAD(P)H | $2 \times 10^{-7}$   | 60                | 4                 | [46] |
|                |                                 | Thiophenols                  | $2 \times 10^{-6}$   | 45                | 2                 | [45] |
|                | MIP-covered electrode           | Amoxicillin                  | $0.3 \times 10^{-6}$ | 20                | -                 | [39] |
|                |                                 | Metoprolol                   | $1.3 \times 10^{-7}$ | 14                | -                 | [40] |
|                | MIP TiO <sub>2</sub> thin films | Acids                        | $5 \times 10^{-4}$   | 300               | -                 | [43] |
|                |                                 |                              | $5 \times 10^{-5}$   | 300               | -                 | [44] |
|                |                                 | AMP <sup>1</sup>             | $1.5 \times 10^{-5}$ | 60                | -                 | [44] |
| GMP            |                                 | $1.5 \times 10^{-5}$         |                      |                   |                   |      |
| CMP            | $8 \times 10^{-7}$              |                              |                      |                   |                   |      |

Table 1. Cont.

| Transducer            | Receptor                         | Analyte          | LOD (mol/L)           | Response Time (s)     | Stability (Weeks) | Ref  |      |
|-----------------------|----------------------------------|------------------|-----------------------|-----------------------|-------------------|------|------|
| Impedimetric          | MIP layer on Au electrode        | Phenylalanine    | $3 \times 10^{-3}$    | 900                   | -                 | [33] |      |
|                       |                                  | Glucose          | $50 \times 10^{-6}$   | -                     | <1                | [49] |      |
|                       | MIP film                         | Nicotine         | $0.5 \times 10^{-6}$  | 600                   | 12                | [25] |      |
|                       | MIP film                         | Theophylline     | $1 \times 10^{-6}$    | 600                   | -                 | [50] |      |
|                       | MIP on Au electrode              | Resorcinol       | $0.1 \times 10^{-6}$  | -                     | 5                 | [51] |      |
|                       | MIP particles on Au electrode    | Imidacloprid     | $4.61 \times 10^{-6}$ | -                     | -                 | [52] |      |
| Conductometric        | Multiplex MIP on gold electrodes | AMP <sup>2</sup> | $50 \times 10^{-6}$   | -                     | -                 | [53] |      |
|                       |                                  | NFA <sup>3</sup> | $20 \times 10^{-6}$   | -                     | -                 |      |      |
|                       |                                  | BMK <sup>4</sup> | $20 \times 10^{-6}$   | -                     | -                 |      |      |
| Conductometric        | MIPs into membranes              | Atrazine         | $0.5 \times 10^{-6}$  | 1800                  | 16                | [54] |      |
|                       | MIPs                             | Haloacetic acids | $3 \times 10^{-9}$    | 30                    | 12                | [55] |      |
| Voltametric           | MIP NPs                          | Morphine         | $0.3 \times 10^{-3}$  | -                     | -                 | [56] |      |
|                       | MIP films                        | Ephedrine        | $0.5 \times 10^{-3}$  | -                     | -                 | [57] |      |
|                       | MIP                              | Paracetamol      | $7.9 \times 10^{-7}$  | -                     | -                 | [58] |      |
|                       | MIP                              | Dopamine         | $1.98 \times 10^{-9}$ | 4                     | 1                 | [59] |      |
|                       | MIP                              | Atrazine         | $1 \times 10^{-6}$    | 600                   | -                 | [60] |      |
|                       | MIP                              | Creatinine       | $1.23 \times 10^{-3}$ | 120                   | <1                | [61] |      |
|                       | MIP-based electrode              | Sol-gel film     | Melamine              | $0.83 \times 10^{-9}$ | -                 | 4    | [62] |
|                       |                                  |                  | TATP <sup>5</sup>     | $27 \times 10^{-6}$   | -                 | -    | [24] |
|                       | MIP(DA) <sup>6</sup> films       | Sol-gel film     | TNT <sup>7</sup>      | $0.1 \times 10^{-9}$  | -                 | -    | [63] |
|                       |                                  |                  | RDX <sup>8</sup>      | $10 \times 10^{-9}$   | -                 | -    |      |
| MIP-covered electrode | Sol-gel film                     | Cholestanol      | $1 \times 10^{-12}$   | -                     | 7                 | [64] |      |

<sup>1</sup> AMP: adenosine monophosphate; GMP: guanosine monophosphate; CMP: cytidine monophosphate; <sup>2</sup> AMP: amphetamine; <sup>3</sup> NFA: N-formyl amphetamine; <sup>4</sup> BMK: benzyl methyl ketone; <sup>5</sup> TATP: triacetone triperoxide; <sup>6</sup> MIP(DA): molecularly imprinted polydopamine; <sup>7</sup> TNT: 2,4,6-trinitrotoluene; <sup>8</sup> RDX: Research Department explosive or 1,3,5-trinitroperhydro-1,3,5-triazine.

## 2.2. Conductometric and Impedimetric Sensors

Conductometric and impedimetric sensors were also adapted to include MIPs as a recognition layer, which also ensures the selectivity. Conductometric sensors are based on a time-dependent change in conductivity triggered by the binding event and are less popular than potentiometric ones. In their design, two main setups can be distinguished. The first approach was reported by Mosbach et al. [65]. In their work, a membrane selective for benzyltriphenylphosphonium ions was pressing the bare polymer particles onto a polished surface connected to two Pt-wires and fixed on a filter paper. An alternative approach was proposed by Piletsky et al. [54], where a MIP membrane was placed between two Pt-electrodes in a conventional electrochemical cell with separated compartments. Since conductometric devices are in general poorly selective, especially in buffers due to the high ionic strength, reference NIP (non-imprinted polymers)-based sensors are always needed. This type of device can be upgraded by using interdigitated electrodes, which allow for a more reliable comparison between MIPs and NIPs [55].

Impedimetric sensors are based on the measurement of an alternated current generated by the binding interaction towards the selective membrane compared to the applied alternating current on the system. The measurement relies on the change of the total electrical resistance and reactance to the flow of the applied current through the given medium. Depending on the sensing principle, impedimetric sensors can be classified into two major subclasses: resistive and capacitive [66]. Capacitive sensors are nowadays widely used, especially those that provide a near-ideal capacitor behavior, with a phase angle close to 90°. To fulfill this condition, the imprinted polymer layer has to be electrically insulated and the binding event has to take place very close to the transducer. The insulation condition can be easily achieved with (meth)acrylic MIPs. For the second condition, thin films are preferred because they provide better performance than thick films. Indeed, thin films concentrate all the available binding sites close to the transducer and thus improve

the sensitivity. It has also been reported that electropolymerized thin layers (around 10–50 nm) do not usually provide a convenient insulation because of the presence of local defects in the polymer matrix. Hence, special treatments with “blocking agents” such as alkanethiols for gold transducers have been shown to conveniently enhance insulation, thus improving sensor performance [33]. A wide variety of molecules have been detected using impedimetric sensors: phenylalanine [33], nicotine [25], glucose [49], theophylline [50], melamine [62], resorcinol [51], imidacloprid [52], and amphetamine [53] (see Table 1 for the characteristics of these sensors).

MIP interfacing with a transducer can be made either with SAMs [67], as previously mentioned, or by grafting photopolymerization [68]. The trend of miniaturization and mass production led to the development of interdigitated capacitance sensors, e.g., for amino acids [69] and protein allergens [70].

### 2.3. Voltametric and Amperometric Sensors

The last type of electrochemical sensors that we describe in this tutorial review is represented by voltammetric and amperometric sensors, which are currently extensively used. The measured signal corresponds to the current flow as primary transduction phenomenon, so these sensors are considered to be faradaic coupled devices. A potential is applied between the sensor and a reference electrode in a three-electrode setup. The flow through the counter electrode and the sensor is continuously measured to produce an analytical signal. Electroactive targets are required for both types of sensors. Non-electroactive analytes can nevertheless be detected, but an electroactive probe such as ferro-ferricyanide is required in that case. The detection requires the analyte to diffuse close enough to the transducer in order to undergo an electron transfer. Since there is no physical contact between the analyte and the transducer, the electron transfer has to be mediated by the sensing element, and conductive MIPs are particularly suited for such sensors.

The correct integration of MIPs into an electrode is crucial, and various strategies, such as embedding nanoparticles into polymer matrixes, deposition by sol–gel chemistry, and mixing with graphite as a paste to form electrodes, have been explored. Electropolymerized films have been used to embed particles into electrodes. The direct grafting or electropolymerization onto an electrode also represents a convenient approach. To increase conductivity and obtain a better signal, graphite powder [33] and nanoparticles [71–73] have been included in these sensors. Morphine [21,56], ephedrine [57], paracetamol [58], dopamine [59,71], homovanillic acid [74], atrazine [60], creatinine [61], cholestanol [64], triacetone triperoxide [24], 2,4,6-trinitrotoluene, and 1,3,5-trinitroperhydro-1,3,5-triazine explosives [63] (see Table 1 for the characteristics of these sensors) are representative analytes. The analytic results obtained for the detection of creatinine using a MIP-based sensor showed comparable precision and accuracy with results obtained by HPLC [61]. We should note that voltammetry is the most selective electrochemical technique because it can specifically detect the analyte thanks to its intrinsic properties such as specific oxidation and reduction peaks. Kröger et al. developed one of the first imprinted polymer-based sensor using screen-printed electrodes and differential pulse voltammetry [75]. Several types of voltammetric sensors can be distinguished based on the shape of their applied potential function. The most commonly used are linear sweep voltammetry and cyclic voltammetry sensors. The applied potential shape varies either linearly with time (for linear sweep voltammetry and cyclic voltammetry) or as constant increments on a linear ramp (for differential pulse voltammetry) or as square wave function (for square wave voltammetry), respectively. These techniques generally improve the signal-to-noise ratio and therefore the sensitivity.

### 3. Mass-Sensitive Sensors

All sensors that generate their signal thanks to a mass change leading to a measurable, reliable, and analytical frequency response are considered mass-sensitive sensors. The piezoelectric effect, discovered in 1880 by Pierre and Jacques Curie brothers [76], is the basis

of all mass-sensitive devices. Examples of such sensors for MIPs include, as mentioned above, MEMS alone [47] or MEMS combined with cantilevers [77], as well as extensively used piezoelectric sensors such as quartz crystal microbalance (QCM) or surface acoustic wave (SAW) sensors, which are described in the following subsections.

### 3.1. QCM Sensors

One of the most used mass-sensitive sensors in the MIP community are QCM sensors. Their signal is generated by a decrease of the oscillation frequency of a piezoelectric crystal upon the recognition of the template by the MIP. The change in frequency is herein proportional to the square of the fundamental resonance frequency mode and can be used for quantitative readouts according to the Sauerbrey equation. A scheme of a QCM chip and the corresponding sensogram are shown in Scheme 2a. QCM sensors have been widely used for the detection of steroid hormones such as nandrolone [78] and neurotransmitters such as catecholamines [79], as well as for other analytes like the  $\beta$ -blocking drug (S)-propranolol [80], caffeine [81], trichlorfon [82],  $\alpha$ -amanitin [83], N-hexanoyl-L-homoserine lactone [84], and L-tryptophan [85]. The experimental characteristics of the sensors detecting these analytes are summarized in Table 2. Molecularly imprinted films on top of a QCM can be made using the drop-casting by embedding the preformed MIP nanoparticles (NPs) into a polymer matrix [78,79], covalent immobilizing via coupling reactions [84], in situ polymerizing [80], or imprinting onto preformed polymers [81,82].

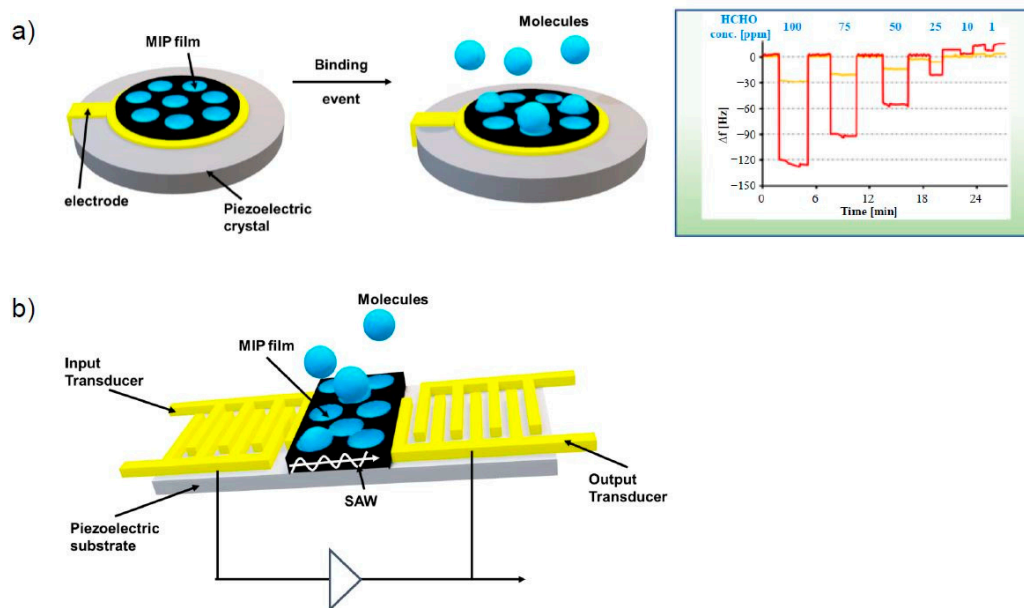
**Table 2.** MIP-based mass-sensitive sensors.

| Transducer | Receptor                   | Analyte                            | LOD (mol/L)                                      | Response Time (s) | Stability (Weeks) | Ref          |
|------------|----------------------------|------------------------------------|--|-------------------|-------------------|--------------|
| QCM        | MIP film                   | (S)-propranolol                    | $50 \times 10^{-6}$                              | -                 | -                 | [80]         |
|            | MIP membranes              | Caffeine                           | $1 \times 10^{-6}$                               | 720               | -                 | [81]         |
|            | Two formats <sup>1</sup>   | Catecholamines                     | -  | 150               | -                 | [79]         |
|            | MIP film                   | Trichlorfon                        | $4.63 \times 10^{-6}$                            | -                 | 3                 | [82]         |
|            | MIP film                   | Formaldehyde                       | $1 \times 10^{-6}$                               | 10                | -                 | [86]         |
|            | MIP NPs                    | N-hexanoyl-L-homoserine lactone    | $1 \times 10^{-6}$                               | 1800              | -                 | [84]         |
|            | MIP film onto QCM crystal  | $\alpha$ -Amanitin<br>L-tryptophan | $0.052 \times 10^{-12}$<br>$0.73 \times 10^{-6}$ | 1200<br>5         | poor<br>-         | [83]<br>[85] |
| SAW        | MIP particles <sup>2</sup> | Phenacetin                         | $5 \times 10^{-9}$                               | 900               | -                 | [87]         |
|            | MIP film                   | IgG                                | $0.4 \times 10^{-9}$                             | 1020              | -                 | [88]         |
|            | MIP film onto SAW chip     | Sulfamethizole                     | $1.7 \times 10^{-9}$                             | 1000              | -                 | [89]         |
|            | MIP film onto Au electrode | Glyphosate                         | $1 \times 10^{-12}$                              | 1800              | -                 | [90]         |
|            | MIP film                   | CDNF protein                       | $4.2 \times 10^{-6}$                             | 1980              | -                 | [91]         |

<sup>1</sup> Crushed and sieved particles and film; <sup>2</sup> Crushed and sieved particles embedded in a PVC matrix.

### 3.2. SAW Sensors

SAW sensors represent another example of mass-sensitive readouts (see Scheme 2b). They are made of one or more comb-like interdigitated electrodes and rely on the propagation of mechanical vibrations on a piezoelectric surface material. In practice, like for Rayleigh waves, the effect of the surface acoustic waves is produced by an electric signal at resonance frequency [92]. Quantitative measurements are obtained by adding a sensitive layer on top, which produces an alternating voltage. These sensors are used for the detection of various analytes ranging from proteins [88] to small molecules [87]. Recent applications include the detection of biomarkers for early stage diagnosis and/or therapy monitoring (notably in neurodegenerative diseases) [91], antibiotics [89], and herbicides [90] (see Table 2 for the MIPs used and the experimental characteristics of the sensors). The simplicity of handling, real-time detection, and good sensitivity are the main advantages of SAW sensors. Despite their complicated electronics circuits, which remain a primary limitation, their relatively low cost has rendered the SAW sensors more and more compatible with an industrial-scale production [93].



**Scheme 2.** (a) Scheme of a quartz crystal microbalance (QCM) chip coated with a MIP film (left) and a typical QCM response (right) for a MIP thin film (red), as well as the non-imprinted polymer (yellow) at different vapor concentrations of formaldehyde (in blue on the top of the graph). The difference between the red and yellow curves is attributed to the mass effects induced by the incorporation of the analyte into the recognition sites of the polymer film. The time-phase evolution corresponds to the change in formaldehyde concentration. Response graph taken with permission from [86]. (b) Scheme of a surface acoustic wave (SAW) sensor.

#### 4. Optical Sensors

Optical sensors are extensively used in various fields such as biotechnology, environmental monitoring, pharmaceuticals, and clinical analysis. In luminescent optical sensors, the detection method relies on the conversion of a binding event into a measurable light thanks to fluorescence, chemiluminescence, or colorimetric changes; these light signal changes lead to highly sensitive, flexible, and inexpensive sensors. The signal transduction can occur in three different ways:

- The inherent optical activity of the target.
- The incorporation of a fluorophore or a chromophore into the polymer matrix, which can result either in the quenching or in the enhancement of fluorescence.
- A signal generated upon a catalytic reaction, leading to spectroscopically active species.

The following subsections describe the different types of readouts used for optical MIP sensors: UV/Vis absorption, fluorescence, surface plasmon resonance (SPR), localized SPR (LSPR), surface-enhanced Raman scattering (SERS), surface-enhanced Raman resonance scattering (SERRS), reflectometric interference, and colorimetric.

##### 4.1. UV/Vis and Fluorescence Readout

UV/Vis absorption is one of the simplest readouts based on a change in the absorption spectrum of the sensing element induced by the analyte [94]. The response is quick and provides a quantitative information on the binding itself, but the technique suffers from low sensitivity. Nevertheless, if the analyte shows a specific absorption peak in the monitored region, this technique provides a further level of accuracy and could overall enhance the selectivity of the sensor. Examples include the chemical grafting of MIPs onto the surface of polystyrene microplates for rapid binding assays [95] or in combination with solid-phase extraction, as one of the most common uses, for example for the detection of propranolol in biological fluids [96].

Sensitivity can be increased by combining the imprinted polymers with different nanostructures like quantum dots, which modify their luminescent properties upon a



physical or chemical interaction (i.e., binding event) occurring close enough to their surface [97,98]. High sensitivity, selectivity, and low detection limits can be achieved when fluorescence readouts are used for optical MIP sensors [99,100]. A fluorescent readout can be easily coupled with optical waveguides [101] and is compatible with a variety of fluorescent probes like quantum dots [97,102], upconverting particles (UCP) [103], and fluorescent derivatives [104] (see Table 3 for the detected analytes and the experimental characteristics of the sensors). In the case of clenbuterol analyte, the accuracy of fluorescence detection was validated by comparative analysis with other methods [103]. When non-fluorescent analytes are targeted, fluorescence quenching or enhancement can be achieved upon the addition of fluorescent materials or dyes such as fluorescent functional monomers [105,106] into the polymer matrix. Several types of analytes have been detected by optical MIP sensors with fluorescent readouts: small or organic molecules (caffeine [107], cocaine [108]), proteins [109], and inorganic ions (Al (III) [110] or Ag (I) [105]).

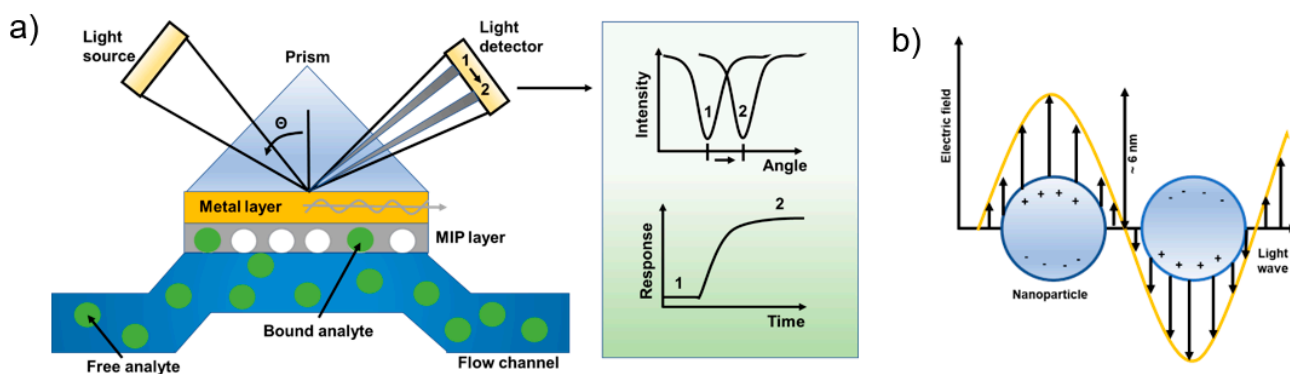
**Table 3.** MIP-based optical sensors.

| Transducer              | Receptor   | Analyte                       | LOD (mol/L)  | Response Time (s) | Stability (Weeks) | Ref   |
|-------------------------|--|-------------------------------|--|-------------------|-------------------|-------|
| UV/Vis and fluorescence | 3-Aminophenyl boronic acid film                                  | Epinephrine                   | $9.2 \times 10^{-6}$   | 1200              | -                 | [95]  |
|                         | Crushed and sieved MIP particles                                 | Propranolol                   | $0.32 \times 10^{-3}$  | -                 | -                 | [96]  |
|                         | Crushed and sieved MIP particles                                 | Al <sup>3+</sup>              | $3.62 \times 10^{-6}$  | 40                | -                 | [110] |
|                         | Core shell composite particles                                   | 4-nitrophenol                 | $76 \times 10^{-9}$  | -                 | -                 | [98]  |
|                         | QDs <sup>1</sup> embedded in MIP films/NPs                       | Amylase, lipase, lysozyme     | $0.1 \times 10^{-3}$ ,<br>$0.1 \times 10^{-3}$ ,<br>$0.013 \times 10^{-3}$ | 300               | -                 | [109] |
|                         | MIP particles embedded in a PVC <sup>2</sup> matrix              | Deltamethrin                  | $0.018 \times 10^{-3}$   | 180               | 3                 | [97]  |
|                         | MIP tip on an optical fiber                                      | Cocaine                       | $2 \times 10^{-6}$   | ~1000             | 4                 | [108] |
|                         | MIP tip on an optical fiber                                      | 2,4-D <sup>3</sup>            | $0.25 \times 10^{-9}$  | 600               | -                 | [106] |
|                         | Crushed and sieved MIP particles                                 | Caffeine                      | $1.22 \times 10^{-3}$  | 4800              | -                 | [107] |
|                         | MIP ionic liquid CdSe/ZnS QDs                                    | Mycotoxin zearalenone         | $3.12 \times 10^{-6}$  | -                 | -                 | [111] |
|                         | MIP NPs embedded in a PVA <sup>4</sup> film, on an optical fiber | 2,4-D <sup>3</sup> , Citrinin | $1 \times 10^{-9}$ ,<br>$1 \times 10^{-6}$                                 | 600               | -                 | [101] |
|                         | Core-shell composite MIP particles                               | Clenbuterol                   | $0.12 \times 10^{-6}$  | 300               | -                 | [103] |
| MIP NPs                 | Trypsin  | $50 \times 10^{-12}$          | 7200   | -                 | [104]             |       |
| SPR                     | MIP film spin-coated on the SPR chip                             | Ammonium perfluorooctanoate   | $0.13 \times 10^{-6}$  | 600               | -                 | [112] |
|                         | MIP NPs coupled on a SPR chip                                    | $\beta$ -lactoglobulin        | $211 \times 10^{-12}$  | -                 | -                 | [113] |
|                         | MIP film on a SPR chip   | Aflatoxin B1                  | $1.04 \times 10^{-9}$  | 300               | 12                | [114] |
|                         | MIP film spin-coated on the SPR chip                             | Ochratoxin A                  | $0.028 \times 10^{-6}$   | 600               | -                 | [115] |
| LSPR                    | Au NPs embedded in an MIP gel                                    | Adrenaline                    | $5 \times 10^{-6}$   | long              | -                 | [116] |
|                         | Supra-particles between MIP-NPs and BPA-Au-NPs                   | Bisphenol A (BPA)             | $<10^{-9}$   | 1200              | -                 | [117] |
| SERS/SERRS              | Core-shell Au@MIP particles                                      | (S)-propranolol               | $1 \times 10^{-7}$   | 1                 | -                 | [118] |
|                         |  | Mercaptobenzoic acid          | $1 \times 10^{-15}$  | -                 | -                 | [119] |
| Reflectometric          | MIP films  | Atrazine                      | $8 \times 10^{-6}$   | 2000              | -                 | [120] |
| Colorimetric            | MIPC <sup>5</sup>  | Methyl phosphonic acid        | $1 \times 10^{-6}$   | 480               | -                 | [121] |
|                         | Silver-halide holograms into MIPs films                          | Testosterone                  | $1 \times 10^{-6}$   | long              | -                 | [122] |

<sup>1</sup> QDs: quantum dots; <sup>2</sup> PVC: polyvinyl chloride; <sup>3</sup> 2,4-D: 2,4-dichlorophenoxyacetic acid; <sup>4</sup> PVA: polyvinyl alcohol; <sup>5</sup> MIPC: molecularly imprinted photonic crystals.

#### 4.2. SPR Readout

Transducers based on SPR use the change in thickness and the refractive index of thin films coupled to metal surfaces to generate an analytical signal upon binding. The metal surfaces supporting surface plasmons are typically gold and silver, but copper, titanium, and chromium are suitable alternatives. Surface plasmons represent an optical excitation effect based on the theory of attenuated total reflection originally developed by Kretschmann and Raether [123] and Otto [124] that is widely used in sensors. Polarized light is hereby applied onto a prism covered with a thin layer of metal, such as gold, which generates a surface plasmon. After interfacing the MIP with the transducer, the analyte binding to the MIP leads to an incidence angle shift that is concentration-dependent (see Scheme 3a) because the analyte binding changes the refractive index of the MIP layer. Surface integration is achieved upon the coupling of presynthesized MIP using thiols [113], by the in situ polymerization of thin films [114,115] (see Table 3 for the detected analytes and the experimental characteristics of the sensors), or by electropolymerization.



**Scheme 3.** (a) Scheme of a surface plasmon resonance sensor setup (left). Polarized light is applied onto a prism covered with a thin layer of metal, such as gold, which generates a surface plasmon. Analyte binding events induce changes on the surface and consequently a resonance angle shift (right, top) that can be transformed into a sensogram either directly or by the intensity change at a fixed angle (right, bottom graph). (b) Scheme of localized surface plasmon resonance (LSPR), where the free conduction electrons of the metal nanoparticle oscillate due to their strong coupling with the incident light. Adapted with permission from [125]. The electromagnetic field decay length in LSPR is around 6 nm compared to 200 nm in SPR.

Since conductive compounds propagate the plasmonic wave and increase sensitivity [126–128], metallic nanoparticles such as Au-NPs and Au-nanostars are often embedded into MIP matrices. For more information on these devices, one can refer to the minireview of Lépinay et al. covering the years 2010–2011 [129] or the recent review by Malik et al. [130]. SPR sensors have been successfully used for the detection of a wide range of molecules from proteins to small molecules like explosives; therefore, sensing techniques based on SPR sensors are relatively common. Recently, fiber optic SPR techniques using molecularly imprinted polymers for the detection of perfluorinated compounds in water have also been reported [112].

#### 4.3. LSPR Readout

LSPR is an optical phenomenon produced by the collective oscillation of valence electrons and the following absorption of the incident photons in the UV/Vis band (conduction band) of a noble metal nanostructure (see Scheme 3b). The technique was extensively reviewed by Hammond and coworkers, who illustrated its applications in material science and biosensing [125]. Possible metal surfaces are palladium (Pd), platinum (Pt), gold (Au), and silver (Ag). The sensing signal is based on the refractive index change near their surface. The readout can be based on UV–Vis spectroscopy by monitoring a wavelength-shift of the collective oscillation due to changes of the refractive index during the binding event.

For example, it has been shown [131] that the intense color of an aqueous gold nanoparticles solution is an expression of the LSPR phenomenon. Matsui et al. [116] proposed the colorimetric detection of adrenaline by a MIP using acrylic acid as a functional monomer. Gold nanoparticles were embedded into the polymer matrix. The plasmon absorption band at 522 nm in water was shifted down to 511 nm in the presence of 1 mM adrenaline due to the increased average distance between NPs following the template uptake. The blue shift was shown to be concentration dependent and allowed for the measurement of concentrations as low as 5  $\mu$ M. “Supra-particles” consisting of MIP nanoparticles (MIP-NPs) and template-functionalized gold nanoparticles (template-Au-NPs) were instead used by Takeuchi’s group to measure bisphenol A (BPA) in ethyl acetate [117] (see Table 3 for the detected analytes and the experimental characteristics of the LSPR sensors). In their elegant approach, MIP-NPs and BPA-surface coated Au-NPs were allowed to spontaneously assemble thanks to the MIP–BPA affinity. Incubation with increasing concentrations of free BPA resulted in the progressive disassembly of supra-particles due to the competitive binding with MIP-NPs. Such disassembly could be easily tracked by measuring the changes in the plasmon peak.

#### 4.4. SERS and SERRS Readouts

Another readout method is the observation of enhanced electromagnetic fields generated by a nanostructured surface, such as those of SERS and SERRS, and monitoring the changes in these enhanced fields during binding events [125]. SERS and SERRS readouts can be used in two ways: in conjunction with LSPR, as mentioned above, or by using the specific vibrational spectrum of Raman active molecules. SERS/SERRS is one of the latest integrated transduction methods into MIP-based sensors. SERS is a surface-sensitive technique based on the enhancement of Raman scattering during the binding event promoted by the coupling between the incident laser and localized surface plasmons on rough metal structures or nanostructures. The mechanism is not yet fully understood, so two options have been discussed in the literature: an electromagnetic theory related to the LSPR phenomenon around the NPs and a charge-transfer complex due to a chemical bond formation between the analyte and the metal structure that would increase its polarizability [118]. The SERRS phenomenon appears when the laser is close to a metal NP’s surface, resulting in hotspots on the surface and consequently the production of a clear signal that varies with the laser position relative to the nanoparticle [132]. Our group successfully detected the drug propranolol by micro-Raman spectroscopy on single MIP microspheres [133]. Rather low limits of detection have been reached on single MIP particles ( $100 \times 10^{-6}$  M) and single MIP microspheres ( $1 \times 10^{-6}$  M). The limit of detection was improved by three orders of magnitude when SERS measurements were performed on single Au-MIP composites particles, where the analyte could even be detected in diluted equine serum [118]. Compared to fluorescence-based sensors, SPR and SERS sensors show limits of detection in the femtomolar range [111,119], which is around five orders of magnitude lower than fluorescence. Additionally, Raman spectroscopy allows for the measurement of the specific vibrational spectrum of a molecule (i.e., its fingerprint), thus contributing to its identification. SERS sensors can be enhanced by using composite particles with gold colloids, which behave as nano-antennae forming hot spots [118,128].

#### 4.5. Reflectometric Interference Readout

Reflectometric interference spectroscopic sensors are used in fiber optical or planar waveguide setups by recording the interference occurring between two beams propagating through different optical paths in a single or two different fibers/waveguides (beam split and beam combining) [120,134]. In such devices, molecularly imprinted polymers have been used as a recognition layer and were either embedded as nanoparticles in films or directly synthesized as a film on the surface. The transducer system is based on a multi-layer design consisting of a silica (glass) layer followed by a high-refractive Ta<sub>2</sub>O<sub>5</sub> layer and an additional silica layer that can be chemically modified. Belmont et al. [120] used

this type of sensor for the detection of atrazine pesticide in toluene (see Table 3 for the experimental characteristics of the sensor). The MIP layer was created by spin-coating of the precursors followed by in situ polymerization, as well as by the auto-assembly of MIP nanoparticles using an associative linear polymer as the matrix.

#### 4.6. Colorimetric Readout

In addition to classical optical sensors, there are devices based on structural colored materials such as holograms and photonic crystals. In 2012, Liu et al. [121] proposed a molecularly imprinted photonic crystal against the degradation products of nerve agents (organophosphorus compounds). They used polymethyl methacrylate colloid particles for the preparation of a packed colloidal crystal array embedded in an imprinted hydrogel. The analyte was detected by diffraction. Silver-halide reflection holograms represent another example of structural-based optical transducers. The optochemical sensor was fabricated by inscribing a hologram inside a molecularly imprinted polymer film made of acrylates [122]. Upon testosterone binding, a wavelength shift of the reflection peak was measured and translated into an analytical signal. Regarding the MIP-based transmission holographic sensors, the response time upon template binding is rather long, since 8 h of incubation are necessary to well-discriminate the imprinted from the non-imprinted-based sensor. Similar results were obtained for template (S)-propranolol.

### 5. Interfacing

The interfacing of a MIP onto a transducer is one of the most crucial steps for sensor preparation. As mentioned before, this depends on the sensor surface and the chosen readout. MIPs are normally interfaced based on two different physical forms: (1) thin films and (2) pre-synthesized microparticles/nanoparticles. Micro or nanoparticles can be interfaced in several ways: embedded into polymer matrices [34] with core-shell designs and covalent linkage to the surface [135] or drop-casting [136], spin-coating [137], and spray-coating directly onto the surface [138].

For electrochemical sensors, particles are often embedded into membranes or polymer matrices. As mentioned before, a commonly used polymer matrix is polyvinyl chloride (PVC), especially for ISEs [34] as membranes, but it is also possible to spin-coat a thin non-conductive layer of PVC onto a transducer [78]. Gels are an alternative to embed powders into polymer matrixes, such as with herbicides [75] or morphine [139]. Another possibility is to add MIP particles into a prepolymerization mixture of electropolymerizable monomers and then carry out the polymerization directly on the sensor surface [56]. Electropolymerizable monomers include dopamine, pyrrole, thiophene, and 4-aminthiophenol. For the embedding into a polymer matrix, an adhesive layer can also be deposited by spin-coating onto the transducer surface, and the particles can be entrapped by stamping using a polydimethylsiloxane (PDMS) stamp. Subsequently, heat is applied, and the particles sink into the adhesive layer [140]. If necessary, the polymer layer can be tailored to be conductive to enhance the signal. For electrochemical sensors, mixing with graphene powder or carbon paste was shown to be a suitable way to increase the conductivity of (meth)acrylic MIP powders [41]. The particles are mixed with a conducting material (e.g., carbon nanotubes, graphene, graphite, or carbon black) and a binder (e.g., paraffin or PVC) to yield a paste, and then they are formed into electrodes for use. Alternatively to the above physical means, a covalent coupling to the sensor surface can also be carried out. This method is often used on gold surfaces due to their easy reaction with thiols [141] or on silica after silanization [135,142] that provides amino, epoxy, or even carboxy groups on the chips depending on the chosen silane. These groups can easily be coupled with nanoparticles carrying either amino- or carboxy-groups on their surface, which are obtained by including specific functional monomers directly into the polymerization medium or by creating a functionalized shell around presynthesized MIP particles. However, the main drawback of this technique is the often incomplete surface coverage. Thus, deactivation and blocking steps are necessary to avoid any unspecific reading from the uncoated spots,

which makes this approach less convenient than the direct deposition of continuous thin films. In addition, reproducibility is limited because the number of particles per chip and, hence, the overall sensitivity can vary.

As previously stated, thin films can be obtained by free radical polymerization [129] or electropolymerization of monomers deposited by drop-casting, spin-coating, or through self-assembled monolayers (SAMs) [67]. In 2013, a review about signal enhancement on thin films using different interfacing techniques was published by Kutner's group [143], who presented the advantages of interfacing homogeneous layers rather than discrete particles.

The most applied MIPs are based on poly(meth)acrylates, which can be grafted onto the surface in order to create thin films by either thermal- or photo-initiated polymerization, the last being the most commonly used and easiest to handle. In both cases, a covalent immobilization of the initiator (surface initiation) or of a monomer [144] is necessary. In some cases, the thickness of the layer can be tuned by just varying the polymerization time if controlled polymerization techniques are used (i.e., reversible-deactivation radical polymerizations). Another way to use photo-polymerization, the top-down approach, is to spread a pre-polymerization mixture containing a photo-initiator via spin-coating [137] or drop-casting without rotation [136] onto a transducer. Spin-coating and drop-casting also apply to imprinted films via sol-gel chemistry. As such, dip-coating and spray-coating can be found in the literature for the formation of MIP films on electrodes and optical fibers. As mentioned above, SAMs [42] can be used for transducer modification.

The last interfacing method is the direct polymerization on electrochemical transducers via electropolymerization in the presence of a template. The resulting polymers can be either conductive or non-conductive. The morphology and thickness can be easily tuned by the selection of suitable solvents, electrolytes, and the number of deposition cycles (in general, cyclic voltammetry is used for the deposition). The only limitation of the technique comes from the restricted panel of electropolymerizable monomers (e.g., 3-aminophenylboronic acid, thiophenes, aniline, phenol, 1,2-phenylenediamine, 2-aminothiophenol/4-aminothiophenol, pyrrole, and dopamine [25,58,145–147]) and therefore the number of functional groups capable to stabilize the template.

## 6. Conclusions and Future Prospects

Over the past few decades, MIPs have gained a prominent role as sensing components in the design of chemosensors, notably to obtain an improved selectivity. The ability to design chemosensors capable of detecting various analytes explains their wide range of applications, which include medical diagnosis, environmental and industrial monitoring, toxicological analysis, and the detection of explosives and chemical warfare agents. In the future, the requirements imposed by the use of MIP-based chemosensors in medical or industrial applications will become even more stringent in terms of selectivity, sensitivity, miniaturization, and simplicity of use. Such applications are expected to continuously stimulate the development of MIP-based (chemo)sensors.

In this review, we provided an overview of the various chemosensing devices based on the use of MIPs together with interfacing approaches and applications. Despite the significant progress already achieved in this field, further innovations are expected to come from the development of new transduction elements or the improvement of current ones, especially in terms of sensitivity. Similarly, improvements are also expected on the MIP side, not only with the introduction of new interfacing strategies but also with MIPs capable of responding to external stimuli like pH, light, or temperature and new MIP design methods able to precisely control their thickness and their organization into predefined patterns (i.e., micro- and nano-structuring of MIPs). This particular approach is regarded as a way of simultaneously turning a MIP into a sensing element and a transducer. Therefore, similarly to optical chemosensors based on imprinted photonic crystals, the polymer structure will be in charge of both target recognition and signal generation.

All these improvements are expected to lead to the detection of an even broader range of analytes, as well as to the development of more compact, more stable chemosensors

and perhaps at much lower costs, in order to render them accessible to underdeveloped countries, notably for their use in environmental and healthcare monitoring applications. Paper-based sensors are an example of such economic MIP-based chemosensors.

**Author Contributions:** Writing—original draft preparation, N.L., L.D., and C.G.; writing—review and editing, L.D., C.G. and K.H.; visualization, N.L. and L.D.; supervision, L.D. and C.G.; project administration and funding acquisition, K.H. All authors have read and agreed to the published version of the manuscript.

**Funding:** This work was financially supported by the European Commission (project NOSY for New Operational Sensing systems, Grant agreement ID 653839, H2020-EU.3.7).

**Institutional Review Board Statement:** Not applicable.

**Informed Consent Statement:** Not applicable.

**Acknowledgments:** CNRS and University of Technology of Compiègne are acknowledged for administrative and technical support.

**Conflicts of Interest:** The authors declare no conflict of interest.

## References

1. Ye, L.; Haupt, K. Molecularly imprinted polymers as antibody and receptor mimics for assays, sensors and drug discovery. *Anal. Bioanal. Chem.* **2004**, *378*, 1887–1897. [CrossRef]
2. Hayden, O.; Lieberzeit, P.A.; Blaas, D.; Dickert, F.L. Artificial antibodies for bioanalyte detection—Sensing viruses and proteins. *Adv. Funct. Mater.* **2006**, *16*, 1269–1278. [CrossRef]
3. Hayden, O. One binder to bind them all. *Sensors* **2016**, *16*, 1665. [CrossRef]
4. Uzun, L.; Turner, A.P.F. Molecularly-imprinted polymer sensors: Realising their potential. *Biosens. Bioelectron.* **2016**, *76*, 131–144. [CrossRef]
5. Dickert, F.L. Molecular imprinting and functional polymers for all transducers and applications. *Sensors* **2018**, *18*, 327. [CrossRef] [PubMed]
6. Lowdon, J.W.; Diliën, H.; Singla, P.; Peeters, M.; Cleij, T.J.; van Grinsven, B.; Eersels, K. MIPs for commercial application in low-cost sensors and assays—An overview of the current status quo. *Sens. Actuators B Chem.* **2020**, *325*. [CrossRef] [PubMed]
7. Chen, L.; Wang, X.; Lu, W.; Wu, X.; Li, J. Molecular imprinting: Perspectives and applications. *Chem. Soc. Rev.* **2016**, *45*, 2137–2211. [CrossRef]
8. Haupt, K.; Rangel, P.X.M.; Tse, B.; Bui, S. Molecularly imprinted polymers: Antibody mimics for bioimaging and therapy. *Chem. Rev.* **2020**. [CrossRef] [PubMed]
9. Bedwell, T.S.; Whitcombe, M.J. Analytical applications of MIPs in diagnostic assays: Future perspectives. *Anal. Bioanal. Chem.* **2016**, *408*, 1735–1751. [CrossRef]
10. Hulanicki, A.; Glab, S.; Ingman, F. Chemical sensors definitions and classification. *Pure Appl. Chem.* **1991**, *63*, 1247–1250. [CrossRef]
11. Lu, W.; Xue, M.; Xu, Z.; Dong, X.; Xue, F.; Wang, F.; Wang, Q.; Meng, Z. Molecularly imprinted polymers for the sensing of explosives and chemical warfare agents. *Curr. Org. Chem.* **2015**, *19*, 62–71. [CrossRef]
12. Awino, J.K.; Zhao, Y. Molecularly imprinted nanoparticles as tailor-made sensors for small fluorescent molecules. *Chem. Commun.* **2014**, *50*, 5752–5755. [CrossRef] [PubMed]
13. Xiao, W.; Xiao, M.; Fu, Q.; Yu, S.; Shen, H.; Bian, H.; Tang, Y. A portable smart-phone readout device for the detection of mercury contamination based on an aptamer-assay nanosensor. *Sensors* **2016**, *16*, 1871. [CrossRef] [PubMed]
14. Baş, D. Sensitive and reliable paper-based glucose sensing mechanisms with smartphone readout using the:  $L * a * b * color$  space. *Anal. Methods* **2017**, *9*, 6698–6704. [CrossRef]
15. Gao, X.; Wu, N. Smartphone-Based Sensors, *Electrochem. Soc. Interface*. Available online: <https://www.electrochem.org/ecs-blog/25-years-interface-2/> (accessed on 29 April 2021).
16. Broeders, J.; Croux, D.; Peeters, M.; Beyens, T.; Duchateau, S.; Cleij, T.J.; Wagner, P.; Thoelen, R.; De Ceuninck, W. Mobile application for impedance-based biomimetic sensor readout. *IEEE Sens. J.* **2013**, *13*, 2659–2665. [CrossRef]
17. Guembe-García, M.; Santaolalla-García, V.; Moradillo-Renuncio, N.; Ibeas, S.; Reglero, J.A.; García, F.C.; Pacheco, J.; Casado, S.; García, J.M.; Vallejos, S. Monitoring of the evolution of human chronic wounds using a ninhydrin-based sensory polymer and a smartphone. *Sens. Actuators B Chem.* **2021**, *335*, 129688. [CrossRef]
18. Wang, J.; Liang, R.; Qin, W. Molecularly imprinted polymer-based potentiometric sensors. *Trends Anal. Chem.* **2020**, *130*, 115980. [CrossRef]
19. Mahmoudpour, M.; Torbati, M.; Mousavi, M.M.; de la Guardia, M.; Ezzati Nazhad Dolatabadi, J. Nanomaterial-based molecularly imprinted polymers for pesticides detection: Recent trends and future prospects. *Trends Anal. Chem.* **2020**, *129*, 115943. [CrossRef]
20. Zdrachek, E.; Bakker, E. Potentiometric sensing. *Anal. Chem.* **2021**, *93*, 72–102. [CrossRef]

21. Kriz, D.; Mosbach, K. Competitive amperometric morphine sensor based on an agarose immobilised molecularly imprinted polymer. *Anal. Chim. Acta* **1995**, *300*, 71–75. [[CrossRef](#)]
22. Liang, R.; Zhang, R.; Qin, W. Potentiometric sensor based on molecularly imprinted polymer for determination of melamine in milk. *Sens. Actuators B Chem.* **2009**, *141*, 544–550. [[CrossRef](#)]
23. Goud, K.Y.; M, S.; Reddy, K.K.; Gobi, K.V. Development of highly selective electrochemical impedance sensor for detection of sub-micromolar concentrations of 5-Chloro-2,4-dinitrotoluene. *J. Chem. Sci.* **2016**, *128*, 763–770. [[CrossRef](#)]
24. Mamo, S.K.; Gonzalez-Rodriguez, J. Development of a molecularly imprinted polymer-based sensor for the electrochemical determination of triacetone triperoxide (TATP). *Sensors* **2014**, *14*, 23269–23282. [[CrossRef](#)] [[PubMed](#)]
25. Liu, K.; Wei, W.Z.; Zeng, J.X.; Liu, X.Y.; Gao, Y.P. Application of a novel electrosynthesized polydopamine-imprinted film to the capacitive sensing of nicotine. *Anal. Bioanal. Chem.* **2006**, *385*, 724–729. [[CrossRef](#)] [[PubMed](#)]
26. Thévenot, D.R.; Toth, K.; Durst, R.A.; Wilson, G.S. Electrochemical biosensors: Recommended definitions and classification. *Anal. Lett.* **2001**, *34*, 635–659. [[CrossRef](#)]
27. Antuña-Jiménez, D.; Díaz-Díaz, G.; Blanco-López, M.C.; Lobo-Castañón, M.J.; Miranda-Ordieres, A.J.; Tuñón-Blanco, P. *Molecularly Imprinted Electrochemical Sensors: Past, Present, and Future*; Li, S., Piletsky, S.A., Ge, Y., Lunec, J., Eds.; ScienceDirect: Amsterdam, The Netherlands, 2012; ISBN 9780444563316.
28. Hedborg, E.; Winquist, F.; Lundström, I.; Andersson, L.I.; Mosbach, K. Some studies of molecularly-imprinted polymer membranes in combination with field-effect devices. *Sens. Actuators A. Phys.* **1993**, *37–38*, 796–799. [[CrossRef](#)]
29. Piletsky, S.A.; Turner, A.P.F. Electrochemical sensors based on molecularly imprinted polymers. *Electroanalysis* **2002**, *14*, 317–323. [[CrossRef](#)]
30. Sharma, P.S.; Pietrzyk-Le, A.; D'Souza, F.; Kutner, W. Electrochemically synthesized polymers in molecular imprinting for chemical sensing. *Anal. Bioanal. Chem.* **2012**, *402*, 3177–3204. [[CrossRef](#)]
31. Blanco-López, M.C.; Lobo-Castañón, M.J.; Miranda-Ordieres, A.J.; Tuñón-Blanco, P. Electrochemical sensors based on molecularly imprinted polymers. *TrAC Trends Anal. Chem.* **2004**, *23*, 36–48. [[CrossRef](#)]
32. Grieshaber, D.; MacKenzie, R.; Vörös, J.; Reimhult, E. Electrochemical biosensors - Sensor principles and architectures. *Sensors* **2008**, *8*, 1400–1458. [[CrossRef](#)]
33. Panasyuk, T.L.; Mirsky, V.M.; Piletsky, S.A.; Wolfbeis, O.S. Electropolymerized molecularly imprinted polymers as receptor layers in capacitive chemical sensors. *Anal. Chem.* **1999**, *71*, 4609–4613. [[CrossRef](#)]
34. Prasada Rao, T.; Kala, R. Potentiometric transducer based biomimetic sensors for priority envirototoxic markers-An overview. *Talanta* **2008**, *76*, 485–496. [[CrossRef](#)] [[PubMed](#)]
35. Prasad, K.; Kala, R.; Prasada Rao, T.; Naidu, G.R.K. Ion imprinted polymer based ion-selective electrode for the trace determination of dysprosium(III) ions. *Anal. Chim. Acta* **2006**, *566*, 69–74. [[CrossRef](#)]
36. Prasad, K.; Prathish, K.P.; Gladis, J.M.; Naidu, G.R.K.; Rao, T.P. Molecularly imprinted polymer (biomimetic) based potentiometric sensor for atrazine. *Sens. Actuators B Chem.* **2007**, *123*, 65–70. [[CrossRef](#)]
37. Hutchins, R.S.; Bachas, L. Nitrate-selective electrode developed by electrochemically mediated imprinting/doping of polypyrrole. *Anal. Chem.* **1995**, *67*, 1654–1660. [[CrossRef](#)]
38. Kamel, A.H.; Moreira, F.T.C.; Almeida, S.A.A.; Sales, M.G.F. Novel potentiometric sensors of molecular imprinted polymers for specific binding of chlormequat. *Electroanalysis* **2008**, *20*, 194–202. [[CrossRef](#)]
39. Guerreiro, J.R.L.; Sales, M.G.F.; Moreira, F.T.C.; Rebelo, T.S.R. Selective recognition in potentiometric transduction of amoxicillin by molecularly imprinted materials. *Eur. Food Res. Technol.* **2011**, *232*, 39–50. [[CrossRef](#)]
40. Tehrani, M.S.; Vardini, M.T.; Azar, P.A.; Husain, S.W. Molecularly imprinted polymer based PVC-membrane-coated graphite electrode for the determination of metoprolol. *J. Iran. Chem. Soc.* **2010**, *7*, 759–769. [[CrossRef](#)]
41. Javanbakht, M.; Fard, S.E.; Abdouss, M.; Mohammadi, A.; Ganjali, M.R.; Norouzi, P.; Safaraliev, L. A biomimetic potentiometric sensor using molecularly imprinted polymer for the cetirizine assay in tablets and biological fluids. *Electroanalysis* **2008**, *20*, 2023–2030. [[CrossRef](#)]
42. Wang, Y.; Zhou, Y.; Sokolov, J.; Rigas, B.; Levon, K.; Rafailovich, M. A potentiometric protein sensor built with surface molecular imprinting method. *Biosens. Bioelectron.* **2008**, *24*, 162–166. [[CrossRef](#)]
43. Lahav, M.; Kharitonov, A.B.; Katz, O.; Kunitake, T.; Willner, I. Tailored chemosensors for chloroaromatic acids using molecularly imprinted TiO<sub>2</sub> thin films on ion-sensitive field-effect transistors. *Anal. Chem.* **2001**, *73*, 720–723. [[CrossRef](#)]
44. Zayats, M.; Lahav, M.; Kharitonov, A.B.; Willner, I. Imprinting of specific molecular recognition sites in inorganic and organic thin layer membranes associated with ion-sensitive field-effect transistors. *Tetrahedron* **2002**, *58*, 815–824. [[CrossRef](#)]
45. Pogorelova, S.P.; Kharitonov, A.B.; Willner, I.; Sukenik, C.N.; Pizem, H.; Bayer, T. Development of ion-sensitive field-effect transistor-based sensors for benzylphosphonic acids and thiophenols using molecularly imprinted TiO<sub>2</sub> films. *Anal. Chim. Acta* **2004**, *504*, 113–122. [[CrossRef](#)]
46. Pogorelova, S.P.; Zayats, M.; Bourenko, T.; Kharitonov, A.B.; Lioubashevski, O.; Katz, E.; Willner, I. Analysis of NAD(P)<sup>+</sup>/NAD(P)H cofactors by imprinted polymer membranes associated with ion-sensitive field-effect transistor devices and Au-quartz crystals. *Anal. Chem.* **2003**, *75*, 509–517. [[CrossRef](#)] [[PubMed](#)]
47. Tsai, H.H.; Lin, C.F.; Juang, Y.Z.; Wang, I.L.; Lin, Y.C.; Wang, R.L.; Lin, H.Y. Multiple type biosensors fabricated using the CMOS BioMEMS platform. *Sens. Actuators B Chem.* **2010**, *144*, 407–412. [[CrossRef](#)]

48. Kamel, A.H.; Jiang, X.; Li, P.; Liang, R. A paper-based potentiometric sensing platform based on molecularly imprinted nanobeads for determination of bisphenol A. *Anal. Methods* **2018**, *10*, 3890–3895. [[CrossRef](#)]
49. Cheng, Z.; Wang, E.; Yang, X. Capacitive detection of glucose using molecularly imprinted polymers. *Biosens. Bioelectron.* **2001**, *16*, 179–185. [[CrossRef](#)]
50. Wang, Z.; Kang, J.; Liu, X.; Ma, Y. Capacitive detection of theophylline based on electropolymerized molecularly imprinted polymer. *Int. J. Polym. Anal. Charact.* **2007**, *12*, 131–142. [[CrossRef](#)]
51. Kumar Prusty, A.; Bhand, S. Molecularly imprinted polyresorcinol based capacitive sensor for sulphanilamide detection. *Electroanalysis* **2019**, *31*, 1797–1808. [[CrossRef](#)]
52. El-Akaad, S.; Mohamed, M.A.; Abdelwahab, N.S.; Abdelaleem, E.A.; De Saeger, S.; Beloglazova, N. Capacitive sensor based on molecularly imprinted polymers for detection of the insecticide imidacloprid in water. *Sci. Rep.* **2020**, *10*, 14479. [[CrossRef](#)]
53. De Rycke, E.; Leman, O.; Dubruel, P.; Hedström, M.; Völker, M.; Beloglazova, N.; De Saeger, S. Novel multiplex capacitive sensor based on molecularly imprinted polymers: A promising tool for tracing specific amphetamine synthesis markers in sewage water. *Biosens. Bioelectron.* **2021**, *178*. [[CrossRef](#)] [[PubMed](#)]
54. Piletsky, S.A.; Piletskaya, E.V.; Elgersma, A.V.; Yano, K.; Karube, I.; Parhometz, Y.P.; El'skaya, A.V. Atrazine sensing by molecularly imprinted membranes. *Biosens. Bioelectron.* **1995**, *10*, 959–964. [[CrossRef](#)]
55. Suedee, R.; Intakong, W.; Dickert, F.L. Molecularly imprinted polymer-modified electrode for on-line conductometric monitoring of haloacetic acids in chlorinated water. *Anal. Chim. Acta* **2006**, *569*, 66–75. [[CrossRef](#)]
56. Ho, K.C.; Yeh, W.M.; Tung, T.S.; Liao, J.Y. Amperometric detection of morphine based on poly(3,4-ethylenedioxythiophene) immobilized molecularly imprinted polymer particles prepared by precipitation polymerization. *Anal. Chim. Acta* **2005**, *542*, 90–96. [[CrossRef](#)]
57. Mazzotta, E.; Picca, R.A.; Malitesta, C.; Piletsky, S.A.; Piletska, E.V. Development of a sensor prepared by entrapment of MIP particles in electrosynthesised polymer films for electrochemical detection of ephedrine. *Biosens. Bioelectron.* **2008**, *23*, 1152–1156. [[CrossRef](#)]
58. Özcan, L.; Şahin, Y. Determination of paracetamol based on electropolymerized-molecularly imprinted polypyrrole modified pencil graphite electrode. *Sens. Actuators B Chem.* **2007**, *127*, 362–369. [[CrossRef](#)]
59. Li, J.; Zhao, J.; Wei, X. A sensitive and selective sensor for dopamine determination based on a molecularly imprinted electropolymer of o-aminophenol. *Sens. Actuators B Chem.* **2009**, *140*, 663–669. [[CrossRef](#)]
60. Shoji, R.; Takeuchi, T.; Kubo, I. Atrazine sensor based on molecularly imprinted polymer-modified gold electrode. *Anal. Chem.* **2003**, *75*, 4882–4886. [[CrossRef](#)]
61. Patel, A.K.; Sharma, P.S.; Prasad, B.B. Development of a creatinine sensor based on a molecularly imprinted polymer-modified sol-gel film on graphite electrode. *Electroanalysis* **2008**, *20*, 2102–2112. [[CrossRef](#)]
62. Shamsipur, M.; Moradi, N.; Pashabadi, A. Coupled electrochemical-chemical procedure used in construction of molecularly imprinted polymer-based electrode: A highly sensitive impedimetric melamine sensor. *J. Solid State Electrochem.* **2018**, *22*, 169–180. [[CrossRef](#)]
63. Leibl, N.; Duma, L.; Gonzato, C.; Haupt, K. Polydopamine-based molecularly imprinted thin films for electro-chemical sensing of nitro-explosives in aqueous solutions. *Bioelectrochemistry* **2020**, *135*. [[CrossRef](#)]
64. Jalalvand, A.R.; Zangeneh, M.M.; Jalili, F.; Soleimani, S.; Díaz-Cruz, J.M. An elegant technology for ultrasensitive impedimetric and voltammetric determination of cholestanol based on a novel molecularly imprinted electrochemical sensor. *Chem. Phys. Lipids* **2020**, *229*, 104895. [[CrossRef](#)]
65. Kriz, D.; Kempe, M.; Mosbach, K. Introduction of molecularly imprinted polymers as recognition elements in conductometric chemical sensors. *Sens. Actuators B* **1996**, *33*, 178–181. [[CrossRef](#)]
66. Carminati, M. Advances in high-resolution microscale impedance sensors. *J. Sens.* **2017**, *2017*. [[CrossRef](#)]
67. Yang, L.; Wei, W.; Xia, J.; Tao, H.; Yang, P. Capacitive biosensor for glutathione detection based on electropolymerized molecularly imprinted polymer and kinetic investigation of the recognition process. *Electroanalysis* **2005**, *17*, 969–977. [[CrossRef](#)]
68. Delaney, T.L.; Zimin, D.; Rahm, M.; Weiss, D.; Wolfbeis, O.S.; Mirsky, V.M. Capacitive detection in ultrathin chemosensors prepared by molecularly imprinted grafting photopolymerization. *Anal. Chem.* **2007**, *79*, 3220–3225. [[CrossRef](#)]
69. Belbruno, J.J.; Zhang, G.; Gibson, U.J. Capacitive sensing of amino acids in molecularly imprinted nylon films. *Sens. Actuators B Chem.* **2011**, *155*, 915–918. [[CrossRef](#)]
70. Sontimuang, C.; Suedee, R.; Dickert, F. Interdigitated capacitive biosensor based on molecularly imprinted polymer for rapid detection of Hev b1 latex allergen. *Anal. Biochem.* **2011**, *410*, 224–233. [[CrossRef](#)]
71. Kan, X.; Zhao, Y.; Geng, Z.; Wang, Z.; Zhu, J.J. Composites of multiwalled carbon nanotubes and molecularly imprinted polymers for dopamine recognition. *J. Phys. Chem. C* **2008**, *112*, 4849–4854. [[CrossRef](#)]
72. Zhang, Z.; Hu, Y.; Zhang, H.; Yao, S. Novel layer-by-layer assembly molecularly imprinted sol-gel sensor for selective recognition of clindamycin based on Au electrode decorated by multi-wall carbon nanotube. *J. Colloid Interface Sci.* **2010**, *344*, 158–164. [[CrossRef](#)]
73. Huang, J.; Xing, X.; Zhang, X.; He, X.; Lin, Q.; Lian, W.; Zhu, H. A molecularly imprinted electrochemical sensor based on multiwalled carbon nanotube-gold nanoparticle composites and chitosan for the detection of tyramine. *Food Res. Int.* **2011**, *44*, 276–281. [[CrossRef](#)]



74. Diñeiro, Y.; Menéndez, M.I.; Blanco-López, M.C.; Lobo-Castañón, M.J.; Miranda-Ordieres, A.J.; Tuñón-Blanco, P. Computational predictions and experimental affinity distributions for a homovanillic acid molecularly imprinted polymer. *Biosens. Bioelectron.* **2006**, *22*, 364–371. [[CrossRef](#)]
75. Kröger, S.; Turner, A.P.F.; Mosbach, K.; Haupt, K. Imprinted polymer-based sensor system for herbicides using differential-pulse voltammetry on screen-printed electrodes. *Anal. Chem.* **1999**, *71*, 3698–3702. [[CrossRef](#)] [[PubMed](#)]
76. Curie, J.; Curie, P. Développement par compression de l'électricité polaire dans les cristaux hémihédres à faces inclinées. *Bull. Soc. Fr. Miner.* **1880**, *3*, 90. [[CrossRef](#)]
77. Ayela, C.; Dubourg, G.; Pellet, C.; Haupt, K. All-organic microelectromechanical systems integrating specific molecular recognition—A new generation of chemical sensors. *Adv. Mater.* **2014**, *26*, 5876–5879. [[CrossRef](#)]
78. Percival, C.J.; Stanley, S.; Braithwaite, A.; Newton, M.I.; McHale, G. Molecular imprinted polymer coated QCM for the detection of nandrolone. *Analyst* **2002**, *127*, 1024–1026. [[CrossRef](#)]
79. Ling, T.R.; Yau, Z.S.; Tasi, Y.C.; Chou, T.C.; Liu, C.C. Size-selective recognition of catecholamines by molecular imprinting on silica-alumina gel. *Biosens. Bioelectron.* **2005**, *21*, 901–907. [[CrossRef](#)]
80. Haupt, K.; Noworyta, K.; Kutner, W. Imprinted polymer-based enantioselective acoustic sensor using a quartz crystal microbalance. *Anal. Commun.* **1999**, *36*, 391–393. [[CrossRef](#)]
81. Kobayashi, T.; Murawaki, Y.; Reddy, P.S.; Abe, M.; Fujii, N. Molecular imprinting of caffeine and its recognition assay by quartz-crystal microbalance. *Anal. Chim. Acta* **2001**, *435*, 141–149. [[CrossRef](#)]
82. Dayal, H.; Ng, W.Y.; Lin, X.H.; Li, S.F.Y. Development of a hydrophilic molecularly imprinted polymer for the detection of hydrophilic targets using quartz crystal microbalance. *Sens. Actuators B Chem.* **2019**, *300*, 127044. [[CrossRef](#)]
83. Qiu, X.; Li, Y.; Wang, Y.; Guo, H.; Nie, L. A novel molecularly imprinted nanosensor based on quartz crystal microbalance for specific recognition of  $\alpha$ -amanitin. *Microchem. J.* **2020**, *159*, 105383. [[CrossRef](#)]
84. Guha, A.; Ahmad, O.S.; Guerreiro, A.; Karim, K.; Sandström, N.; Ostanin, V.P.; van der Wijngaart, W.; Piletsky, S.A.; Ghosh, S.K. Direct detection of small molecules using a nano-molecular imprinted polymer receptor and a quartz crystal resonator driven at a fixed frequency and amplitude. *Biosens. Bioelectron.* **2020**, *158*. [[CrossRef](#)]
85. Prabakaran, K.; Jandas, P.J.; Luo, J.; Fu, C.; Wei, Q. Molecularly imprinted poly(methacrylic acid) based QCM biosensor for selective determination of L-tryptophan. *Colloids Surf. A Physicochem. Eng. Asp.* **2021**, *611*, 125859. [[CrossRef](#)]
86. Hussain, M.; Kotova, K.; Lieberzeit, A.P. Molecularly imprinted polymer nanoparticles for formaldehyde sensing with QCM. *Sensors* **2016**, *16*, 1011. [[CrossRef](#)]
87. Tan, Y.; Peng, H.; Liang, C.; Yao, S. New assay system for phenacetin using biomimic bulk acoustic wave sensor with a molecularly imprinted polymer coating. *Sens. Actuators B Chem.* **2001**, *73*, 179–184. [[CrossRef](#)]
88. Tretjakov, A.; Syritski, V.; Reut, J.; Boroznjak, R.; Öpik, A. Molecularly imprinted polymer film interfaced with Surface Acoustic Wave technology as a sensing platform for label-free protein detection. *Anal. Chim. Acta* **2016**, *902*, 182–188. [[CrossRef](#)]
89. Ayankojo, A.G.; Tretjakov, A.; Reut, J.; Boroznjak, R.; Öpik, A.; Rappich, J.; Furchner, A.; Hinrichs, K.; Syritski, V. Molecularly imprinted polymer integrated with a surface acoustic wave technique for detection of sulfamethizole. *Anal. Chem.* **2016**, *88*, 1476–1484. [[CrossRef](#)]
90. Mazouz, Z.; Rahali, S.; Fourati, N.; Zerrouki, C.; Aloui, N.; Seydou, M.; Yaakoubi, N.; Chehimi, M.M.; Othmane, A.; Kalfat, R. Highly selective polypyrrole MIP-based gravimetric and electrochemical sensors for picomolar detection of glyphosate. *Sensors* **2017**, *17*, 2586. [[CrossRef](#)] [[PubMed](#)]
91. Kidakova, A.; Boroznjak, R.; Reut, J.; Öpik, A.; Saarna, M.; Syritski, V. Molecularly imprinted polymer-based SAW sensor for label-free detection of cerebral dopamine neurotrophic factor protein. *Sens. Actuators B Chem.* **2020**, *308*, 127708. [[CrossRef](#)]
92. Rayleigh, L.D.C. On waves propagated along the plane surface of an elastic solid. *Proc. London Math. Soc.* **1886**, *17*, 4–11. [[CrossRef](#)]
93. Chang, K.; Pi, Y.; Lu, W.; Wang, F.; Pan, F.; Li, F.; Jia, S.; Shi, J.; Deng, S.; Chen, M. Label-free and high-sensitive detection of human breast cancer cells by aptamer-based leaky surface acoustic wave biosensor array. *Biosens. Bioelectron.* **2014**, *60*, 318–324. [[CrossRef](#)] [[PubMed](#)]
94. Suriyanarayanan, S.; Cywinski, P.J.; Moro, A.J.; Mohr, G.J.; Kutner, W. Chemosensors based on molecularly imprinted polymers. In *Topics in Current Chemistry: Molecular Imprinting*; Haupt, K., Ed.; Molecular Imprinting: Austin, TX, USA, 2012; pp. 165–265, ISBN 9783642284205.
95. Piletsky, S.A.; Piletska, E.V.; Chen, B.; Karim, K.; Weston, D.; Barrett, G.; Lowe, P.; Turner, A.P.F. Chemical grafting of molecularly imprinted homopolymers to the surface of microplates. Application of artificial adrenergic receptor in enzyme-linked assay for  $\beta$ -agonists determination. *Anal. Chem.* **2000**, *72*, 4381–4385. [[CrossRef](#)] [[PubMed](#)]
96. Mullett, W.M.; Martin, P.; Pawliszyn, J. In-tube molecularly imprinted polymer solid-phase microextraction for the selective determination of propranolol. *Anal. Chem.* **2001**, *73*, 2383–2389. [[CrossRef](#)]
97. Ge, S.; Zhang, C.; Yu, F.; Yan, M.; Yu, J. Layer-by-layer self-assembly CdTe quantum dots and molecularly imprinted polymers modified chemiluminescence sensor for deltamethrin detection. *Sens. Actuators B Chem.* **2011**, *156*, 222–227. [[CrossRef](#)]
98. Liu, J.; Chen, H.; Lin, Z.; Lin, J.M. Preparation of surface imprinting polymer capped Mn-doped ZnS quantum dots and their application for chemiluminescence detection of 4-nitrophenol in tap water. *Anal. Chem.* **2010**, *82*, 7380–7386. [[CrossRef](#)]
99. Lakowicz, J.R. Fluorescence sensing. In *Principles of Fluorescence Spectroscopy*; Lakowicz, J.R., Ed.; Springer: Boston, MA, USA, 2006; pp. 623–673, ISBN 978-0-387-46312-4.

100. Li, Y.; Niu, Q.; Wei, T.; Li, T. Novel thiophene-based colorimetric and fluorescent turn-on sensor for highly sensitive and selective simultaneous detection of Al<sup>3+</sup> and Zn<sup>2+</sup> in water and food samples and its application in bioimaging. *Anal. Chim. Acta* **2019**, *1049*, 196–212. [[CrossRef](#)]
101. Ton, X.A.; Acha, V.; Bonomi, P.; Tse Sum Bui, B.; Haupt, K. A disposable evanescent wave fiber optic sensor coated with a molecularly imprinted polymer as a selective fluorescence probe. *Biosens. Bioelectron.* **2015**, *64*, 359–366. [[CrossRef](#)] [[PubMed](#)]
102. Yao, J.; Zhang, K.; Zhu, H.; Ma, F.; Sun, M.; Yu, H.; Sun, J.; Wang, S. Efficient ratiometric fluorescence probe based on dual-emission quantum dots hybrid for on-site determination of copper ions. *Anal. Chem.* **2013**, *85*, 6461–6468. [[CrossRef](#)]
103. Tang, Y.; Gao, Z.; Wang, S.; Gao, X.; Gao, J.; Ma, Y.; Liu, X.; Li, J. Upconversion particles coated with molecularly imprinted polymers as fluorescence probe for detection of clenbuterol. *Biosens. Bioelectron.* **2015**, *71*, 44–50. [[CrossRef](#)]
104. Xu, J.; Haupt, K.; Tse Sum Bui, B. Core-shell molecularly imprinted polymer nanoparticles as synthetic antibodies in a sandwich fluorimmunoassay for trypsin determination in human serum. *ACS Appl. Mater. Interfaces* **2017**, *9*, 24476–24483. [[CrossRef](#)]
105. Sun, H.; Lai, J.P.; Lin, D.S.; Huang, X.X.; Zuo, Y.; Li, Y.L. A novel fluorescent multi-functional monomer for preparation of silver ion-imprinted fluorescent on-off chemosensor. *Sens. Actuators B Chem.* **2016**, *224*, 485–491. [[CrossRef](#)]
106. Ton, X.A.; Tse Sum Bui, B.; Resmini, M.; Bonomi, P.; Dika, I.; Soppera, O.; Haupt, K. A versatile fiber-optic fluorescence sensor based on molecularly imprinted microstructures polymerized in situ. *Angew. Chem. Int. Ed.* **2013**, *52*, 8317–8321. [[CrossRef](#)] [[PubMed](#)]
107. Rouhani, S.; Nahavandifard, F. Molecular imprinting-based fluorescent optosensor using a polymerizable 1,8-naphthalimide dye as a fluorescence functional monomer. *Sens. Actuators B Chem.* **2014**, *197*, 185–192. [[CrossRef](#)]
108. Nguyen, T.H.; Hardwick, S.A.; Sun, T.; Grattan, K.T.V. Intrinsic fluorescence-based optical fiber sensor for cocaine using a molecularly imprinted polymer as the recognition element. *IEEE Sens. J.* **2012**, *12*, 255–260. [[CrossRef](#)]
109. Lee, M.H.; Chen, Y.C.; Ho, M.H.; Lin, H.Y. Optical recognition of salivary proteins by use of molecularly imprinted poly(ethylene-co-vinyl alcohol)/quantum dot composite nanoparticles. *Anal. Bioanal. Chem.* **2010**, *397*, 1457–1466. [[CrossRef](#)]
110. Ng, S.M.; Narayanaswamy, R. Fluorescence sensor using a molecularly imprinted polymer as a recognition receptor for the detection of aluminium ions in aqueous media. *Anal. Bioanal. Chem.* **2006**, *386*, 1235–1244. [[CrossRef](#)]
111. Fang, G.; Fan, C.; Liu, H.; Pan, M.; Zhu, H.; Wang, S. A novel molecularly imprinted polymer on CdSe/ZnS quantum dots for highly selective optosensing of mycotoxin zearalenone in cereal samples. *RSC Adv.* **2014**, *4*, 2764–2771. [[CrossRef](#)]
112. Cennamo, N.; D'Agostino, G.; Porto, G.; Biasiolo, A.; Perri, C.; Arcadio, F.; Zeni, L. A molecularly imprinted polymer on a plasmonic plastic optical fiber to detect perfluorinated compounds in water. *Sensors* **2018**, *18*, 1836. [[CrossRef](#)]
113. Aurelio, R.D.; Ashley, J.; Rodgers, T.L.; Trinh, L.; Temblay, J.; Pleasants, M.; Tothill, I.E. Development of a NanoMIPs-SPR-based sensor for  $\beta$ -lactoglobulin detection. *Chemosensors* **2020**, *8*, 94.
114. Akgönüllü, S.; Yavuz, H.; Denizli, A. SPR nanosensor based on molecularly imprinted polymer film with gold nanoparticles for sensitive detection of aflatoxin B1. *Talanta* **2020**, *219*, 121219. [[CrossRef](#)]
115. Akgönüllü, S.; Armutcu, C.; Denizli, A. Molecularly imprinted polymer film based plasmonic sensors for detection of ochratoxin A in dried fig. *Polym. Bull.* **2021**, *78*, 1–9.
116. Matsui, J.; Akamatsu, K.; Nishiguchi, S.; Miyoshi, D.; Nawafune, H.; Tamaki, K.; Sugimoto, N. Composite of Au nanoparticles and molecularly imprinted polymer as a sensing material. *Anal. Chem.* **2004**, *76*, 1310–1315. [[CrossRef](#)]
117. Uchida, A.; Kitayama, Y.; Takano, E.; Ooya, T.; Takeuchi, T. Supraparticles comprised of molecularly imprinted nanoparticles and modified gold nanoparticles as a nanosensor platform. *RSC Adv.* **2013**, *3*, 25306–25311. [[CrossRef](#)]
118. Bompert, M.; De Wilde, Y.; Haupt, K. Chemical nanosensors based on composite molecularly imprinted polymer particles and surface-enhanced Raman scattering. *Adv. Mater.* **2010**, *22*, 2343–2348. [[CrossRef](#)] [[PubMed](#)]
119. Chang, L.; Ding, Y.; Li, X. Surface molecular imprinting onto silver microspheres for surface enhanced Raman scattering applications. *Biosens. Bioelectron.* **2013**, *50*, 106–110. [[CrossRef](#)] [[PubMed](#)]
120. Belmont, A.S.; Jaeger, S.; Knopp, D.; Niessner, R.; Gauglitz, G.; Haupt, K. Molecularly imprinted polymer films for reflectometric interference spectroscopic sensors. *Biosens. Bioelectron.* **2007**, *22*, 3267–3272. [[CrossRef](#)] [[PubMed](#)]
121. Liu, F.; Huang, S.; Xue, F.; Wang, Y.; Meng, Z.; Xue, M. Detection of organophosphorus compounds using a molecularly imprinted photonic crystal. *Biosens. Bioelectron.* **2012**, *32*, 273–277. [[CrossRef](#)] [[PubMed](#)]
122. Fuchs, Y.; Kunath, S.; Soppera, O.; Haupt, K.; Mayes, A.G. Molecularly imprinted silver-halide reflection holograms for label-free opto-chemical sensing. *Adv. Funct. Mater.* **2014**, *24*, 688–694. [[CrossRef](#)]
123. Kretschmann, E.; Raether, H. Radiative decay of non radiative surface plasmons excited by light. *Z. Naturforsch. Sect. A J. Phys. Sci.* **1968**, *23*, 2135–2136. [[CrossRef](#)]
124. Otto, A. Excitation of nonradiative surface plasma waves in silver by the method of frustrated total reflection. *Physics (College Park. Md.)* **1968**, *410*, 398–410. [[CrossRef](#)]
125. Hammond, J.L.; Bhalla, N.; Rafiee, S.D.; Estrela, P. Localized surface plasmon resonance as a biosensing platform for developing countries. *Biosensors* **2014**, *4*, 172–188. [[CrossRef](#)] [[PubMed](#)]
126. Cenci, L.; Andreetto, E.; Vestri, A.; Bovi, M.; Barozzi, M.; Iacob, E.; Busato, M.; Castagna, A.; Girelli, D.; Bossi, A.M. Surface plasmon resonance based on molecularly imprinted nanoparticles for the picomolar detection of the iron regulating hormone Hepsidin-25. *J. Nanobiotechnol.* **2015**, *13*, 1–15. [[CrossRef](#)] [[PubMed](#)]

127. Cennamo, N.; Donà, A.; Pallavicini, P.; D'Agostino, G.; Dacarro, G.; Zeni, L.; Pesavento, M. Sensitive detection of 2,4,6-trinitrotoluene by tridimensional monitoring of molecularly imprinted polymer with optical fiber and five-branched gold nanostars. *Sens. Actuators B Chem.* **2015**, *208*, 291–298. [[CrossRef](#)]
128. Wackerlig, J.; Lieberzeit, P.A. Molecularly imprinted polymer nanoparticles in chemical sensing - Synthesis, characterisation and application. *Sens. Actuators B Chem.* **2015**, *207*, 144–157. [[CrossRef](#)]
129. Lépinay, S.; Kham, K.; Millot, M.C.; Carbonnier, B. In-situ polymerized molecularly imprinted polymeric thin films used as sensing layers in surface plasmon resonance sensors: Mini-review focused on 2010–2011. *Chem. Pap.* **2012**, *66*, 340–351. [[CrossRef](#)]
130. Malik, M.I.; Shaikh, H.; Mustafa, G.; Bhangar, M.I. Recent applications of molecularly imprinted polymers in analytical chemistry. *Sep. Purif. Rev.* **2019**, *48*, 179–219. [[CrossRef](#)]
131. Varghese, P.I.; Pradeep, T. *A Textbook of Nanoscience and Nanotechnology*; Tata McGraw-Hill Education: New York, NY, USA, 2003.
132. McNay, G.; Eustace, D.; Smith, W.E.; Faulds, K.; Graham, D. Surface-enhanced Raman scattering (SERS) and surface-enhanced resonance Raman scattering (SERRS): A review of applications. *Appl. Spectrosc.* **2011**, *65*, 825–837. [[CrossRef](#)]
133. Bompert, M.; Gheber, L.A.; De Wilde, Y.; Haupt, K. Direct detection of analyte binding to single molecularly imprinted polymer particles by confocal Raman spectroscopy. *Biosens. Bioelectron.* **2009**, *25*, 568–571. [[CrossRef](#)] [[PubMed](#)]
134. Nopper, D.; Lammershop, O.; Wulff, G.; Gauglitz, G. Amidine-based molecularly imprinted polymers—new sensitive elements for chiral chemosensors. *Anal. Bioanal. Chem.* **2003**, *377*, 608–613. [[CrossRef](#)]
135. Kamra, T.; Chaudhary, S.; Xu, C.; Johansson, N.; Montelius, L.; Schnadt, J.; Ye, L. Covalent immobilization of molecularly imprinted polymer nanoparticles using an epoxy silane. *J. Colloid Interface Sci.* **2015**, *445*, 277–284. [[CrossRef](#)]
136. Mazzotta, E.; Turco, A.; Chianella, I.; Guerreiro, A.; Piletsky, S.A.; Malitesta, C. Solid-phase synthesis of electroactive nanoparticles of molecularly imprinted polymers. A novel platform for indirect electrochemical sensing applications. *Sens. Actuators B Chem.* **2016**, *229*, 174–180. [[CrossRef](#)]
137. Schmidt, R.H.; Mosbach, K.; Haupt, K. A simple method for spin-coating molecularly imprinted polymer films of controlled thickness and porosity. *Adv. Mater.* **2004**, *16*, 719–722. [[CrossRef](#)]
138. Bunte, G.; Hürttlen, J.; Pontius, H.; Hartlieb, K.; Krause, H. Gas phase detection of explosives such as 2,4,6-trinitrotoluene by molecularly imprinted polymers. *Anal. Chim. Acta* **2007**, *591*, 49–56. [[CrossRef](#)] [[PubMed](#)]
139. Kirsch, N.; Honeychurch, K.C.; Hart, J.P.; Whitcombe, M.J. Voltammetric determination of urinary 1-hydroxypyrene using molecularly imprinted polymer-modified screen-printed carbon electrodes. *Electroanalysis* **2005**, *17*, 571–578. [[CrossRef](#)]
140. Horemans, F.; Diliën, H.; Wagner, P.; Cleij, T.J. *MIP-Based Sensor Platforms for Detection of Analytes in Nano- and Micromolar Range*; Elsevier: Amsterdam, The Netherlands, 2012; ISBN 9780444563316.
141. Kamra, T.; Chaudhary, S.; Xu, C.; Montelius, L.; Schnadt, J.; Ye, L. Covalent immobilization of molecularly imprinted polymer nanoparticles on a gold surface using carbodiimide coupling for chemical sensing. *J. Colloid Interface Sci.* **2016**, *461*, 1–8. [[CrossRef](#)] [[PubMed](#)]
142. Korposh, S.; Chianella, I.; Guerreiro, A.; Caygill, S.; Piletsky, S.; James, S.W.; Tatam, R.P. Selective vancomycin detection using optical fibre long period gratings functionalised with molecularly imprinted polymer nanoparticles. *Analyst* **2014**, *139*, 2229–2236. [[CrossRef](#)]
143. Sharma, P.S.; Dabrowski, M.; D'Souza, F.; Kutner, W. Surface development of molecularly imprinted polymer films to enhance sensing signals. *TrAC Trends Anal. Chem.* **2013**, *51*, 146–157. [[CrossRef](#)]
144. Luo, X.; Deng, F.; Luo, S.; Tu, X.; Yang, L. Grafting of molecularly imprinted polymers from the surface of Fe<sub>3</sub>O<sub>4</sub> nanoparticles containing double bond via suspension polymerization in aqueous environment: A selective sorbent for theophylline. *J. Appl. Polym. Sci.* **2010**, *116*, 2658–2667. [[CrossRef](#)]
145. Guo, Z.Z.; Florea, A.; Cristea, C.; Bessueille, F.; Vocanson, F.; Goutaland, F.; Zhang, A.D.; Săndulescu, R.; Lagarde, F.; Jaffrezic-Renault, N. 1,3,5-Trinitrotoluene detection by a molecularly imprinted polymer sensor based on electropolymerization of a microporous-metal-organic framework. *Sens. Actuators B Chem.* **2015**, *207*, 960–966. [[CrossRef](#)]
146. Huynh, T.-P.; Sosnowska, M.; Sobczak, J.W.; KC, C.B.; Nesterov, V.N.; D'Souza, F.; Kutner, W. Simultaneous chronoamperometry and piezoelectric microgravimetry determination of nitroaromatic explosives using molecularly imprinted thiophene polymers. *Anal. Chem.* **2013**, *85*, 8361–8368. [[CrossRef](#)]
147. Riskin, M.; Tel-Vered, R.; Bourenko, T.; Granot, E.; Willner, I. Imprinting of molecular recognition sites through electropolymerization of functionalized Au nanoparticles: Development of an electrochemical TNT sensor based on  $\pi$ -donor-acceptor interactions. *J. Am. Chem. Soc.* **2008**, *130*, 9726–9733. [[CrossRef](#)] [[PubMed](#)]